Attachment C:
Conceptual Model For Defining Natural Analogs for Future Yucca Mountain Volcanism And Expected Consequences

Meghan M. Morrissey

Addendum to EPRI 2006 Internal Report on Igneous Events

Introduction

This report presents an updated version of EPRI's conceptual model for a possible future (< 10^6 yr) igneous event at Yucca Mountain from which natural analogs are defined. The most credible and defensible basis for assigning characteristics to a postulate future volcanic eruption at Yucca Mountain is the geological evidence from recent volcanic events in the region. Field observations and petrologic data (Crowe et al., 1988; Perry et al., 1998; Nicholis and Rutherford, 2002; OCRMW, 2003; BSC, 2004; Valentine et al., 2005) made at basalt centers found in YMR that include Thirsty Mesa, Amargosa Valley, southeast Crater Flat, Buckboard Mesa, Quaternary basalts of Crater Flat, Sleeping Butte, and Lathrop Wells, suggest that a future eruption in YMR will likely be a typical basaltic fissure eruption where < 0.1 km^3 of magma could reach the surface. Lathrop Wells basalt center is considered the best example of a natural analog of a future eruption in the Yucca Mountain region, YMR. EPRI continues to support the hypothesis that any magma that erupts in the Yucca Mountain region within the next 10^6 year will be a low volume (< 0.1 km^3) water bearing, crystallizing basaltic magma with an eruption temperature between 975-1010^{o}C. The expected series of eruptive events for a future igneous event in Yucca Mountain within the next 10^6 yr would be comparable to that at Lathrop Wells basalt center. Recent data published by DOE and academic institutes (i.e. Nicholis and Rutherford, 2002; BSC, 2004; Valentine and others, 2005) on Lathrop Wells basalt center have provided new insight on the interpretation of the eruption history at the center. The report is divided into two sections: summary of Lathrop Wells volcanology and inferred eruption history, and expected scenarios for a future eruption in the Yucca Mountain region.

Figure 1: Geologic setting of the Lathrop Wells basalt center (Fig. 2.8 in Perry et al., 1998). Lathrop Wells main cone (denoted by Qbs within the dark grey area) is located along two sets of fissure (cross-hatched lines). Stars mark sites where distal fall deposits have been found (Perry et al., 1998). Mt and Pb identify locations where Miocene tuff and Pliocene basalt are exposed.

I. Summary of Lathrop Wells Physical Volcanology and Eruption History

Physical Volcanology

The Lathrop Wells basalt center (0.09 km^3; Fig. 1) consists of a large scoria cone and three or four sets of fissures marked by accumulations of spatter, bombs and scoria deposits that represent eroded smaller cones (possibly 3-10 small scoria cones (Crowe et al., 1988)). Multiple eruptive events occurred along two sets of fissures that extend 0.2-2 km. The main scoria cone (Lathrop Wells cone) is 140 m high and has a base of 875 m by 525 m and is roughly 0.018 km^3 in volume. Based on data from a recent petrologic and field study of deposits at Lathrop Wells (Valentine et al., 2005), it has been suggested that the cone may have been built from several distinguishable eruptive events occurring essentially in two phases. The first phase (Fig. 2a) produced the lower portion of the cone (0.006 km^3) comprised of lapilli and bomb sized scoria, ribbon and spindle shaped bombs meter in length (Valentine et al., 2005). This phase began with a fire fountain event that produced a thin (1 m) scoria deposit at the base on the cone containing mostly sideromelane clasts (quenched reddish-brown glass). Overlying this sideromelane rich layer are 4-5 layers of coarsening upward tachylite (crystalline clasts) rich layers (lower portion of the cone) suggesting pulsating eruptive events. The south (0.015 km^3) *aa* lava flow (Fig. 2b) is thought to have occurred contemporaneously with the initial cone building stage. The second phase was the upper cone-building stage that was accompanied by a sustained eruption column from which 0.04 km^3 of mostly tachylite tephra was produced (Fig. 2c). As noted in Valentine et al. (2005), the contact between the upper and lower cone deposits is sharp suggesting a dramatic change in emplacement and eruption mechanisms. The lower cone deposits appear to dip both inward and outward and have characteristic features of grain avalanches (Valentine et al., 2005). The upper cone deposits appear to mantle the lower deposits characteristic of emplacement from fall out and are finer grain then the lower cone deposits (Valentine et al., 2005). The upper cone-building stage also emitted the northeastern (0.015 km^3) lava flow (Fig.

2d). The last eruptive event was a small hydrovolcanic event. The hydrovolcanic event is thought to involve a shallow groundwater source in particularly water stored in the alluvium or sand ramp deposits or pre-volcanic surficial deposits (BSC, 2004).

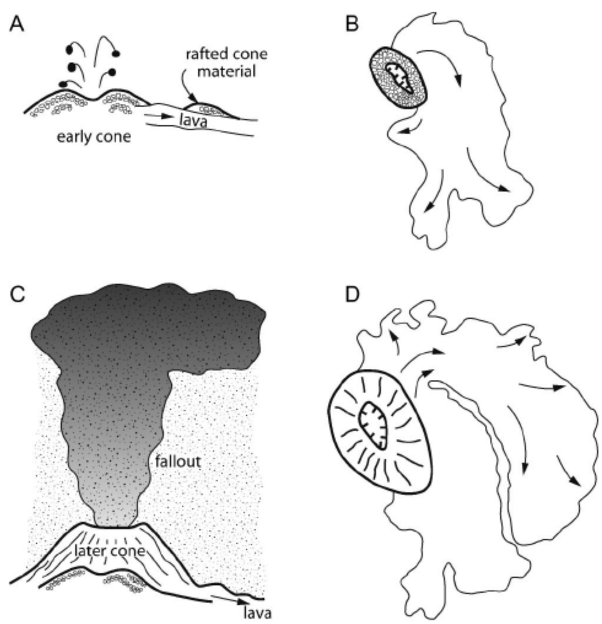

Figure 2: Schematic of (a-d) four possible eruptive events for the main cone at Lathrop Wells basalt center (Valentine et al., 2005).

Clast Analysis

Clast component analyses of scoria deposits from the two phases provide a method for assessing the magma ascent history. For instance, magma that was transported to the earth's surface rapidly then fragmented and quenched while airborne produces reddish-brown basaltic glassy clasts known as sideromelane. Sideromelane droplets are thought to be products of energetic lava fountains or Hawaiian eruptions (Heiken and Wohletz, 1985; BSC, 2004). Magma that was transported to the earth's surface slower and/or stopping along its way will crystallize producing crystalline clasts known as tachylite. Tachylites pyroclasts are microcrystalline textured fragments of basalt that have been described as "quenched crystal" textures (Heiken, 1978). A significant number of samples from scoria deposits at Lathrop Wells were collected and analyzed for clast components by DOE (BSC, 2004). Six different clast types were identified in each sample (BSC, 2004): tachylite, glassy tachylite, sideromelane and crystals (broken olivine, amphibole and/or feldspar phenocrysts) or lithics (tuff or carbonate). Results from this study (BSC, 2004) show that the earliest material erupted produced mostly sideromelane clasts whereas material erupted during the lower and upper cone building phases produced mostly tachylite clasts.

Crystal size measurements of both phenocrysts (> 1 mm) and microlites (< 0.01 mm) can be used to determine ascent rates from results from decompression petrologic experiments (Cashman, 1992; Geschwind and Rutherford, 1995). Isothermal decompression experiments can determine the pressure and temperature conditions of crystal phase equilibrium observed in tephra and lava samples. A study of this type was conducted on tephra and lava samples collected at Lathrop Wells (Nicholis and Rutherford, 2004). According to Nicholis and Rutherford (2004), most of the Lathrop Wells samples contain < 2-4 vol% phenocrysts of olivine and amphibole. The phenocrysts assemblage along with the known water content of < 4.6 wt.% from previous experiments (Luhr and Housh, 2002) suggested a phenocryst-melt equilibrium pressure and temperature of < 175 MPa and 1010^{o}-975^{o}C, respectively (Nicholis and Rutherford, 2004). Plagioclase (An_{69}) is found rarely as microphenocrysts (>0.1 mm) in a crystalline groundmass (microlites) of plagioclase (Nicholis and Rutherford, 2004). The experiments determined that to achieve the crystal size range of the plagioclase microlites observed in the samples, an ascent rate of > 0.04 m/s is required for magma with < 4.6 wt % H_2O (Nicholis and Rutherford, 2004). Equilibrium conditions can also be determined from reactions rims of amphibole (water-bearing mineral) crystals that are very reactive with the liquid phase of magma (melt). The rims of amphiboles in Lathrop Wells' samples suggest a short-lived residence time at a depth roughly 800 m below the surface. At this depth, amphiboles react with the liquid phase of magma to produce the reactions rims visible on amphibole phenocrysts (Nicholis and Rutherford, 2004).

Lathrop Wells Eruption History

The above mentioned petrologic and field data are used by EPRI to derive an eruption history and a magma plumbing system for the Lathrop Wells basalt center. EPRI's eruption history is divided into two phases as recognized by DOE from field deposits (Valentine et al., 2005). Within each phase, a series of eruption styles are described that correspond to eruption products at Lathrop Wells basalt center described by DOE (BSC, 2004; Valentine et al., 2005). The first eruptive phase begins with a series of fissure eruptions that lasted only a few days that transitioned to focused eruptions where the main cone is located. This phase includes the lower cone building deposits and *aa* lava found to the south of the cone. The lower cone building eruption is thought to have formed from Strombolian eruptive events whereas the *aa* lava was eruptive effusively (non-explosive, less energetic than the Strombolian events).

As note by Valentine et al. (2005), the lower cone deposits have characteristic features related to an emplacement and eruption mechanism modeled by McGetchin et al. (1974) as ballistic trajectories of hot fluid fragments of magma. The travel distance is not sufficient to solidify large fragments (bomb size) such that partially welding of ejected material occurs. The model (McGetchen et al., 1974) also considers the accumulation of scoria as rim deposits that may develop into grain avalanches. This model appears to be applicable to the lower cone deposits and is commonly used to describe scoria cone formation. The second phase includes the northern lava flow and the final cone-building event that produced a sustained ash column (Valentine et al., 2005). As note by Valentine et al. (2005), the upper cone deposits have characteristic features unrelated to the ballistic emplacement model (McGetchin et al., 1974). They propose that the magma in the later stages was likely more viscous and fragment similarly to more silicic magmas thus producing the sustained column of finer grain tephra (Valentine et al., 2005).

II. EPRI's Interpretation of the Magma Plumbing System at Lathrop Wells

The magma plumbing system (Figs. 3A-3B) during the first phase is inferred from the relative amount of sideromelane and tachylite clasts found in the respective pyroclastic deposits and crystal content of lavas following a similar approach taken by Corsaro and Pompilio (2004) at Mt. Etna. Lathrop Wells basalts are thought to have originated from 7-8 km depth and transported through the crust in a system of dikes (ICRP, 2002; Nicholis and Rutherford, 2004). Magma that reached the surface first and erupted along the fissures was essentially crystal poor associated with lava fountains. Magma erupted at this time (Fig. 4) is characterized as fragments of molten magma carried by exsolved gases as an annular flow or dispersed flow (Verniolle and Manga, 2000) and was likely partially depleted in volatiles (< 1 wt% H_2O; Holloway and Blank, 1994). This interpretation is based on the presence of sideromelane clasts (quenched glass basalt) found in deposits at the base of the lower portion of the cone (BSC, 2004). To form quenched glass, magma ascended rapidly through the dike to inhibit the formation of microlites then cooled rapidly as it erupted at the surface during the lava fountain phase. The later part of the lower cone building event erupted more crystalline magma based on the predominate appearance of tachylite in the samples from deposits from the lower portion of the cone (BSC, 2004). Magma that reached the surface during the later part of the lower cone building event may have ascended slower allowing crystals to begin nucleating and growing in magma. Tachylite pyroclasts are also thought to form from quench crystallization of fragmented basalt that becomes clogged in the vent during a Strombolian eruptive event (Heiken, 1978). Unlike magma that erupted along the length of the fissure, magma associated with lower cone building Strombolian events erupted from a point source along the fissure. Strombolian style of eruption (characterized by ballistic spatter bombs) are thought to be produced by the expansion and bursting of gas slugs (Fig. 4) at the surface or vent produces the (Verniolle and Manga, 2000). Gas slugs form in rising magma from exsolved volatiles that form bubbles and rise through magma and coalesce to form larger bubbles (slugs) when the bubble fraction reaches at least 70% (Verniolle and Manga, 2000). Slugs are thought to be separated by regions of magma containing bubbles (Verniolle and Manga, 2000).

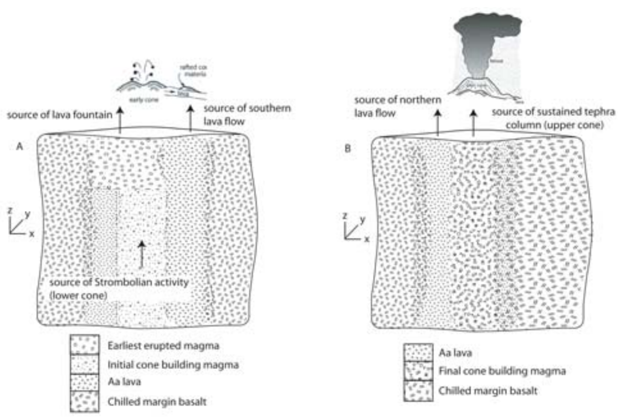

Fig. 3: Schematic drawing of EPRI's conceptual model of the magma plumbing related to the Lathrop Wells basalt center (not to scale).

The transition from a fissure eruption (lava fountains) to a point source or conduit eruption (Strombolian) is thought to occur when magma cools to near its solidus temperature along the dike where the thickness is < 2 m (ICRP, 2003; Delaney and Pollard, 1982). Magma erupted at the surface from the thicker or wider portion of the dike would produce Strombolian activity (Fig. 3A). The contemporaneous occurrence of Strombolian activity and *aa* lava extrusion suggest a lateral variation in crystallization and bubble content along the length of the dike at depth. These two processes are controlled in part by cooling rates. Lava likely extruded from a thinner portion of the dike adjacent to where the conduit developed (Fig. 3A). The thinner regions of the dike (< 2 m) conductive heat loss at the wall rock will induce crystallization of magma (Delaney and Pollard, 1982; Carrigan, 2002) and as magma crystallize it will become more viscous eventually reaching a critical crystal content at which it freezes (Delaney and Pollard, 1982). Exsolved volatiles (bubbles) in magma in the thinner regions of the dike may either move into less viscous magma located in the thicker, hotter, less viscous part of the dike or be released into permeable wall rock.

The second phase includes the northern lava flow and the final cone-building event that produced a sustained ash column (Valentine et al., 2005). From the observed reaction rims on amphiboles from Lathrop Wells samples (Nicholis and Rutherford, 2004), magma erupted during this time may have resided at depths of 800 m for a few days. At this depth, basaltic magma moving up from depth containing < 4.6 wt% H_2O would exsolve at least half of its H_2O (Holloway and Bank, 1984). The slow ascent or stalling of magma in the lower portion of the conduit (Fig. 4) would allow for the formation of microlites as suggested by the tachylite textures in eruptive products associated with this phase. The presence of crystals in magma would increase the viscosity. The ascent from 800 m would exsolve volatiles that would rise at the same rate as the magma (more viscous then earlier magma) thus forming a bubbly or homogenous fluid (Fig. 4; Sparks et al., 1997). As this magma approaches the surface volatiles will continue to exsolve and the magma will begin to fragment into an ash-gas mixture when the bubble fraction reaches roughly 75% (Wilson et al., 1980). The formation and behavior of bubbles in this later more crystalline magma would be similar to that in a silicic magma (Valentine et al., 2005). This process would explain the sustained eruption column (Valentine et al., 2005). During this phase of the eruption, more crystalline degassed magma (< 1 wt% H_2O; Holloway and Blank, 1994) is brought up to the surface at the northern end of the cone producing the later lavas.

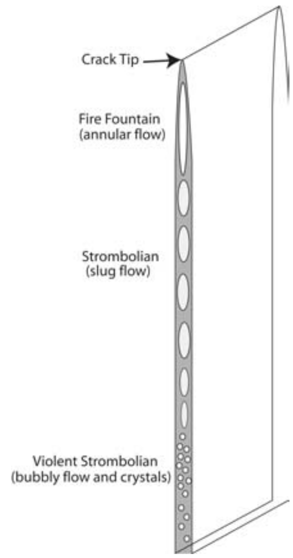

Figure 4: Conceptual model of the change in bubble content with depth in the magma column for Lathrop Wells. Not to scale.

EPRI's interpretation of the magma ascent history at Lathrop Wells becomes important when developing a conceptual model for possible eruptions in the Yucca Mountain region and analysis of dike-drift interaction. Previous models for dike-drift interaction assume magma entering a drift would have a viscosity of the order 1-10 Pa-s capable of filling all drifts and access drifts eventually creating secondary dikes from which magma will erupt at the surface (Woods et al., 2002). Such a model requires that all magma associated with a future eruption at Yucca Mountain remain essentially crystal-free throughout its ascent. As noted in the clast analysis of Lathorp Wells basalt samples, crystallinity of erupted material varies from quenched glass products (sideromelane) that is essentially crystal free to tachylite and crystalline lava that contain abundant microlites. Therefore, a crystal-free magma does not accurately represent Lathrop Wells magma.

Viscosity

EPRI (2006) estimated viscosities for magma in EPRI's conceptual model for the active part of the dike connected to the conduit (Fig. 4). Viscosity values (Fig. 5) for initial crystal-free basalt are available from experimental data for crystal-free, alkali basalt containing up to 5 wt. % H_2O (Murase, 1962; Cas and Wright, 1987) at four temperatures 800°C, 1000°C, 1200°C, and 1400°C (denoted in Fig. 5 by vertical columns of respective symbols) and for H_2O depleted alkali basalt at temperatures between 1100°C to 1500°C (Murase and McBirney, 1973; solid black line in Fig. 5). As demonstrated in Fig. 5, the exsolution of H_2O (due to decompression) from basalt increases the viscosity by 1-2 orders of magnitude depending on temperature. For example, in Fig. 3 at 1000°C and 5 wt. % H_2O the viscosity is approximately 40 Pa-s and at 0 wt. % H_2O the viscosity is 800 Pa-s.

EPRI (2006) estimated viscosity for basalt as a function of crystal content using the Einstein-Roscoe equation (McBirney and Murase, 1984). The Einstein-Roscoe equation estimates an apparent viscosity (η) of magma containing crystals of any size by the following expression:

$$\eta = \eta_o(1-R\phi)^{-2.5}$$

Where η_o is the initial crystal free viscosity, ϕ is the crystal fraction, and R is a constant with a value 1.67 (Griffiths, 2000). The apparent viscosity for Lathrop Wells basalt just below repository depths is estimated at 110 Pa-s (arrow in Fig. 5) using an initial crystal free magma contains 2 wt% H_2O at 1000^oC. Results from this calculation are shown in the inset of Fig. 3. For basalt containing 2 wt. % H_2O, the presence of crystals in basalt increases the viscosity by up to 5 orders of magnitude; 1.1 x10^2 Pa-s to ~6.0 x 10^6 Pa-s for a crystal content increasing from 0 to 0.6. Lava flows tend to terminate their advancement when the crystal content reaches a critical value 0.55-0.6 which corresponds to a viscosity on the order of 10^7 Pa-s (Marsh, 1981; Griffiths, 2000).

For the range of magma rheologies interpreted for the main magma plumbing system (Fig. 4) at Lathrop Wells, Fig. 5 is used to assign a viscosity to each magma rheology. EPRI considers ~40 Pa-s to be a reasonable viscosity for magma ascending from source depth (7-8 km) at Lathrop Wells (magma at this depth is essentially crystal free and contains up to 4.6 wt.% H_2O (Luhr and Housh, 2002; Nicholis and Rutherford, 2004). As magma ascends through the crust it will exsolve volatiles and as it does its viscosity will increase as shown in the black crosses in Fig. 5 assuming magma remains crystal free (Lathrop Wells basalts do contain a negligible amount of phenocrysts, 3-4 vol.%). Magma erupting in the first phase as lava fountains (annular flow) and Strombolian events (slugs and bubble flow alternating) will likely have a viscosity on the order of 10^2 Pa-s. Magma erupting as lava may contain some volatiles (< 1 wt% H_2O; Holloway and Blank, 1994) and will be crystallizing therefore the viscosity will range from 10^3-10^5 Pa-s. Upon decompression, a portion of the remaining H_2O will exsolve forming bubbles that will increase the viscosity by up to an order of magnitude (Pinkerton and Sparks, 1978; Detournay et al., 2003). Decompression induces exsolution of H_2O to the lower pressure that in turn induces undercooling of the magma resulting in quenched crystallization (Sparks and Pinkerton, 1978). EPRI considers 10^3-10^6 Pa-s to be a reasonable range of viscosities for lava at its eruption temperature of 975-1010^oC. Viscosities will rapidly increase several orders of magnitude 10^7-10^8 Pa-s as the lava cools a few 10^oC below its solidus (Griffiths, 2000; Lore et al., 2000) that it is very close to when it erupts. During the second phase of expected eruptive events, a reasonable viscosity for magma before it erupts as a sustained eruption column may be at least 10^3-10^4 Pa-s accounting for microlites and bubbles in the magma.

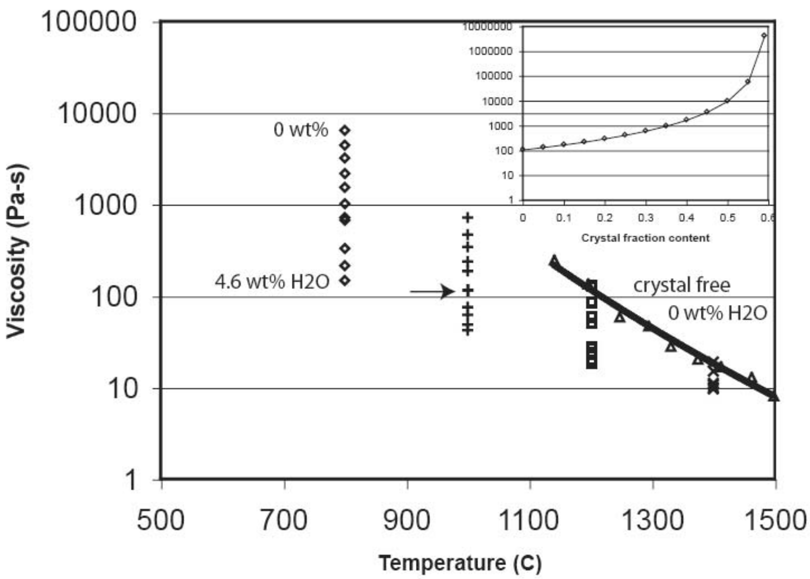

Fig. 5: Viscosity as a function of temperature and H_2O content for crystal free basaltic magma (after Murase, 1962; Cas and Wright, 1987). Inset is viscosity as a function of crystal content calculated using Einstein-Roscoe equation with a crystal free starting viscosity denoted by the arrow.

III. Expected Igneous Consequences Scenarios

The expected extrusive igneous consequences are described in 5 stages. The expected consequences are based on the interpreted eruption history for the Lathrop Wells basalt center.

Extrusive Release Scenarios

Stage 1: Intersection of dike with drift

The first stage of the model considers the ascent of magma through the crust to depths of the proposed repository (300-400 m). The expected sequence of events during magma ascent is based on linear elastic fracture mechanic models for dike propagation (Lister, 1999; Rubin 1995). As discussed by the Igneous Consequence Review Panel (ICRP, 2003), the expected interaction of an ascending sheet dike with a repository drift would involve a < 0.2 m width and 100-200 m long crack tip propagating ahead of the magma filled dike (Fig. 6). Table 1 lists the range of values of characteristic parameters for dikes in the YMR. The ascent rate or propagation rate of a dike has been estimated from decompression experiment to be > 0.04 m/s (Nicholis and Rutherford, 2004). The maximum ascent rate observed at fissure systems in Hawaii and Iceland is 10 m/s (Lister, 1999; Rubin 1995) that provides the upper bound in Table 1.

The width of a future dike in YMR is expected to be < 4 m at depths below 100-125 m from the surface (BSC, 2004). Dike width with respect to depth is constrained from recent field observations of dikes and conduits at monogenetic volcanoes in Nevada and New Mexico (BSC, 2004). Dikes are believed to reach the surface with widths < 4.0 m. As flow activity along a dike (fissure) concentrates at points along the fissure, conduits develop. Magma rising through a conduit will begin to erode the walls by several mechanisms (e.g. thermal erosion, spallation (Valentine and Groves, 1995)) to diameters as large as 125 m, however these diameters develop only in the upper 100-150 m of the surface (BSC, 2004). In EPRI's model, conduit diameters on the order of >10s m are not expected below 100-150 m.

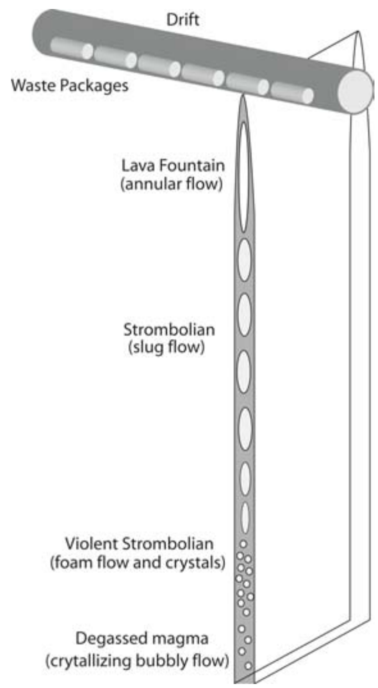

Figure 6: Conceptual model of the change in bubble content with depth in the magma column prior to intersecting a drift. Not to scale. White areas denote gas phase and grey denotes liquid magma. (adapted from Sparks, 1978; Vergniolle and Manga, 2000)

An important part of the conceptual model is the geometry of the crack tip and dike because it provides initial conditions for modeling dike-drift interaction. According to linear elastic models for dikes expected in YMR (ICRP, 2003), the width of a crack tip is expected to be < 0.2 m and when magma reaches the drift the dike will expand to 1.5 m, the mode width of dike found in YMR (OCRWM, 2003). The number of drifts that will be intersected by the dike will depend on the lateral extent of the dike that is expected to be 0.5-5.0 km (Crowe et al., 1983). Following the initial intersection of the dike with a drift, the ascending dike tip can be expected to reach the ground surface above a repository in a matter of minutes (ICRP, 2003; BSC, 2004).

Stage 2: Initial stage magma-drift interaction

Magma that first reaches the repository (Fig. 6) is expected to be similar to that interpreted for the first eruptive phase at Lathrop Wells. EPRI's model suggests that a dike in the Yucca Mountain region is expected to be nonuniform both laterally and vertically with respect to rheology. Magma with the lowest viscosity is expected in the center or the widest part the dike and more crystalline viscous magma is expected along the outer regions or the thinner parts of the dike. The lateral variation in magma properties will produce in general two different styles of expected activity upon entering a drift. Magma may be either a mixture of fragmented magma and gas characteristic of a lava fountain phase or crystallizing magma relatively depleted in volatiles characteristic of *aa* lava. The former type of magma would produce a spray of pyroclastics (scoria, spatter and ribbon bombs) into a drift thereby potentially bombarding and coating waste packages with magma (d1 in Fig. 7A-7B). Spray of magma onto waste packages is not expected to damage waste packages (EPRI, 2005). The latter type of magma would produce a slow moving crystallizing lava flow inside the drift (d2 in Fig. 7A-7B). The lava flow will have a viscosity of 10^3-10^6 Pa-s and will likely flow over or around waste packages forming a chilled margin upon contact with a waste package. Waste packages would be entombed in crystallizing magma (d3 in Fig. 7A-7B).

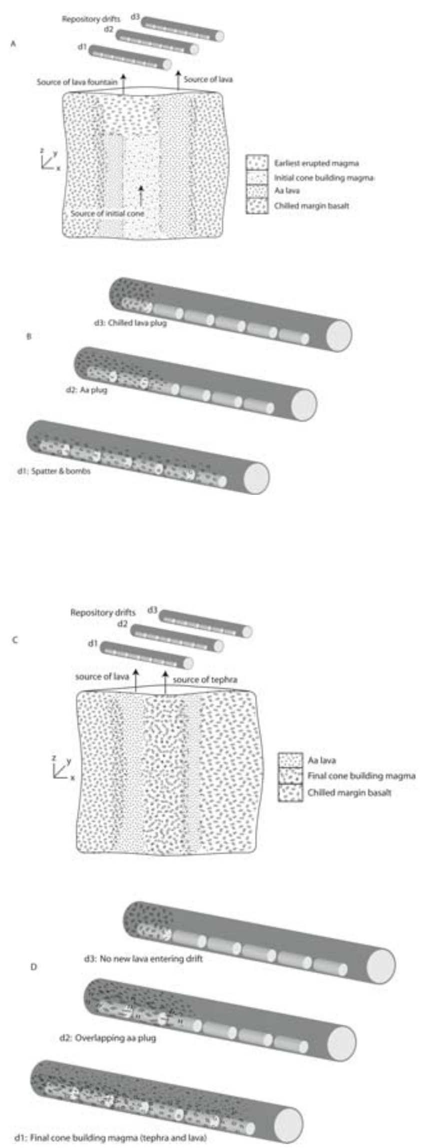

Figure 7: Conceptual model for magma-drift interaction during the (A-B) first three stages and (C-D) and last 2 stages. Not to scale. d1, d2, d3 denote three drifts located along different region of the drift. This model will be updated as new data is made available by DOE and other agencies.

Stage 3: Initial fissure eruption

Magma that is not diverted into the drift will follow the crack tip and make its way to the surface. Magma will erupt at the surface along the fissure as a curtain of lava fountains. The initial width of the dike will be that of the crack tip (< 10 cm) and will gradually increase to 4.0 m the maximum width of fissures in the YMR (OCRWM, 2003). This phase will last hours to several days (ICRP, 2003; Delaney and Pollard, 1982), then eruption activity will localize to 1-3 locations along the fissure.

Magma in the dike will be laterally and vertically gradational with respect to volume fraction of exsolved volatiles, crystallinity and liquid magma as interpreted for Lathrop Wells basalt (Figs. 3A-3B). *Aa* lava that occurred contemporaneous with the initial cone-building phase at Lathrop Wells suggests that part of the magma in the fissure-conduit system was crystallizing and volatile depleted. Therefore, a lateral temperature gradient is expected from the margin of the dike to the center. Assuming that the width of the dike varies laterally, then it is expected that the conduit or cone building part of the eruption would develop at the widest part of the dike where cooling rates are lowest. Lava is expected to erupt along thinner parts of the dike where temperatures are lower due to high rates of heat loss by contact with the wall rock. Volcanic activity is expected to cease along the thinnest (< 1 m wide) parts of the dike within 10 days when temperatures are at or below the solidus temperature due to conductive cooling for alkali basalts similar to Lathrop Wells basalts (ICRP, 2003).

TABLE 1: Summary table of dike characteristics at basaltic centers in the YMR - [ ] denotes mean values (EPRI, 2004).

Width (m)	0.3-4.0 [1.5]
Lateral extent (km)	0.5-5.0
Ascent rate (m/s)	0.04-10 [1]
# Dikes	1-10 [3]
Spacing (m)	100-690
# Vents per dike	1-10 [2-3]
Conduit diameter (m) at surface	1-50 [10]
Conduit diameter (m) at 300 m	1-4

Stage 4: Formation of conduits and central vents

Within hours to 10s days from onset the fissure eruption at the surface will cease and activity will be focused at 1 to 3 conduits (ICRP, 2003). At the repository, drifts that contain spatter and other pyroclastic deposits from an earlier stage, and are connected to the center or the widest part the dike may be inundated by a bubble-magma mixture (Fig. 6 and d3 in Fig.7C-7D). In other drifts that contain spatter or pyroclastic material or lava and located within the narrow regions of the dike crystallizing magma may move into drifts filling space not occupied by volcanic materials (d2 in Fig.7C-7D).

At the surface, material not diverted into the drift will likely produce an ash plume capable of transporting ash > 20 km from the vent to the regulatory compliance boundary. The expected volume of scoria deposited from this phase is 0.01-0.048 km^3 (this includes the fraction of ash size material transported in the plume away from the cone, violent Strombolian event).

During this stage of the eruption, erupted magma may contain radioactive material, either as entrained UO_2 or as radionuclides dissolved into the magma, from the waste packages damaged by the initial interaction with the dike (EPRI, 2004). The mechanical processes that would result in the most damage to the waste packages include the impact of fragments of wall rock and magma from the initial intrusion of the dike into a drift. Thermal erosion of a waste package may arise if a package gets caught in the upward flow of magma. This process may affect at least 1 waste package (1.8 m diameter, 5.0 m length) and possibly two, depending on the width of the dike (0.3 - 4 m) and the location of the dike intersection relative to it.

The amount of radioactive material that may contaminate the magma depends, in part, on the size of the conduit and how magma interacts with waste packages during this prolonged stage (EPRI, 2004). The expected conduit width at future YMR basaltic eruptions is < 4 m at the repository depth (BSC, 2005) and at depths < 100 m the conduit is expected to flare to diameters > 10-50 m (e.g., Piaute Ridge and Basalt Ridge (BSC, 2005)). Waste packages cannot be transported to the surface if the conduit widths are < 2 m. The size of any intact waste package (1.8 m diameter, 5.0 m length), assuming it could be lifted by the flow of magma, will restrict magma transport through a fissure. This constriction in the fissure and sluggish flow of magma will lead to rapid solidification of the dike in this constricted region. Thus, it may be reasonable to suggest that waste packages would only be able to be transported to the surface in dikes with widths at the upper end of the range of YMR dikes (2-4 m).

Stage 5: Final stage magma-drift interaction

The final magma-drift interaction scenarios involve relatively degassed, crystallizing magma. Magma diverted into a drift may overlap earlier *aa* lava that entombed or covered waste packages if there is space otherwise the drift will be sealed off from additional magma (d2 in Fig.7C-7D). If additional magma does enter, this later lava flow is not expected to completely fill the drift. Another scenario is a drift that already is closed off to the conduit by a chilled lava plug (d1 in Fig.7C-7D). No additional lava is expected to enter these drifts.

REFERENCES

BSC, "Characterize Eruptive Processes at Yucca Mountain, Nevada", *MDL-MGR-GS-000005* Las Vegas. Nevada: Bechtel SAIC Company (2004).

BSC (Bechtel SAIC Company), "Magma Dynamics at Yucca Mountain, Nevada", *ANL-MGR-GS-000005 REV 00* (2005).

Cas and Wright, 1987. Volcanic Successions: Modern and ancient. Allen and Unwin Co. London, p. 528,

Cashman, K.V., 1992. Groundmass crystallization of Mount St. Helens dacite, 1980-1986. A tool for interpreting shallow magmatic processes: Contributions to Mineralogy and Petrology. 61: 292-305.

Cashman, K.V., C. Thornber, J.P. Kauahikaua, "Cooling and crystallization of lava in open channels and the transition of pahoehoe lava to *'A'a*", *Bulletin of Volcanology*, **61**, 3, (1999).

Cosaro, R.A. and M. Pompilio, 2004. Magma dynamics in the shallow plumbing system of Mt. Etna as recorded by compositional variations in volcanics of recent summit activity (1995-1999), J. Volcanol. Geotherm Res. 137, p. 55-71.

Crowe, B. S. Self, D. Vaniman, R. Amos, and F. Perry, "Aspects of potential magmatic disruption of a high level radioactive waste repository in southern Nevada", *Journal of Geology*, **91**, 259, (1983).

Crowe, B. C. Harrington, L. McFadden, F. Perry, S. Wells, B. Turrin and D. Champion, "Preliminary geological map of the Lathrop Wells volcanic center", *LA-UR-88-4155*, (1988).

Delaney, P., D. D. Pollard, "Solidification of basaltic magma during flow in a dike", *American Journal of Science,* **282**, 856, (1982).

EPRI, "Potential Igneous Processes Relevant to the Yucca Mountain Repository: Extrusive-Release Scenario, Analysis and Implication", *EPRI Report 1008169* (2004).

EPRI, "Potential Igneous Processes Relevant to the Yucca Mountain Repository: Intrusive-Release Scenario", *EPRI Report 1011165* (2005).

Gerschwind J.E. and MJ Rutherford, 1995. Crystallization of microlites during magma ascent: the fluid mechanics of the 1980-86 eruptions at Mt. St. Helens. Bulletin of Volcanology. 57:356-370.

Griffiths, R.W., 2000. The Dynamics of Lava Flows. Annual Reviews of Fluid Mechanics. 32: 477-518.

Heiken, G. 1978. Characteristics of tephra frm Cinder Cone, Lassen Volcanic National Park California. Bulletin of Volcanology. 41: 119-130.

Heiken G, and Wohletz, K (1985) Volcanic Ash. University of California. Press, 258

Holloway J. and J. Bank, 1994. Applications of experimental results to C-O-H species in natural melts, in Carroll, MR and Holloway, J. eds. Volatiles in magmas: Mineralogical Society of America Reviews in Mineralogy. 30: 187-230.

ICRP, "Final report of the igneous consequences peer review panel", *Bechtel SAIC Company LLC*, pp. 86 (2003).

Lister, J.R., 1990. "Buoyancy driven fluid fracture: the effects of material toughness and of low-viscosity precursors", *Journal of Fluid Mechanics*, 210, 263-280.

Lore, J., H. Gao, A. Aydin, (2000). Viscoelastic thermal stress in cooling basalt flows. Journal of Geophysical Research, vol. 105, p. 23,695-23,709.

Luhr, J.F. and TB Housh, 2002. Melt volatile contents in basalts from Lathrop Wells and Red Cone, Yucca Mountain Region: Insights from glass inclusions: Eos (Transactions, American Geophysical Union), 83: V22A-1221.

Marsh, B. D., (1981). On the crystallinity, probability of occurrence, and rheology of lava and magma. Contrib. Mineral. Petrol. 78: 85-98.

McBirney A. and Murase T, 1984. Rheological properties of magma. A Rev. Earth Planet. Sci. 12:337-357.

McGetchin, T.R.; Settle, M.; and Chouet, B.A. 1974. Cinder Cone Growth Modeled after Northeast Crater, Mount Etna, Sicily. Journal of Geophysical Research, 79:3257-3272.

McBirney A. and Murase T., (1984). Rheological properties of magma. A Rev. Earth Planet. Sci. 12:337-357.

Murase, T., (1962), Viscosity and related properties of volcanic rocks at 800^{o} to 1400^{o}C. Hokkaido Univ. Fac. Sci. J, Ser. 7 1: 487-584.

Murase T and A. McBirney, 1973. Properties of some common igneous rocks and their melts at high temperatures. Geological Society of America Bulletin. 84:3563-3592.

Nicholis, M. and M. Rutherford, "Experimental constraints on magma ascent rate for the Crater Flat volcanic zone hawaiite", *Geology*, **32**, 489 (2004).

OCRWM, "Characterize eruptive processes at Yucca Mountain, Nevada", *ANL-MGR-GS-000002 REV 00.1* (2003).

Perry, F. V., B. M. Crowe, G. A. Valentine, and L. M. Bowker, editors, *Volcanism Studies: Final Report for Yucca Mountain Project, Los Alamos National Laboratories*, LA-13478, Tables 1.2, 2.A and 2.B, December 1998.

Rubin, A., "Propagation of magma-filled cracks", *Annual Review of Earth and Planetary Science*, **23**, 287, (1995).

Sparks, R.S.J.; Bursik, M.I.; Carey, S.N.; Gilbert, J.S.; Glaze, L.S.; Sigurdsson, H.; and Woods, A.W. 1997. *Volcanic Plumes*. New York, New York: John Wiley and Sons. TIC: 247134.

Sparks, R.S.J. and H. Pinkerton, (1978). Effect of degassing on rheology of basaltic lava. Nature. 276: 385-386.

Valentine, G. A., and K. R. Groves 1995. Entrainment of country rock during basaltic eruptions of the Lucero Volcanic Field, New Mexico. Journal of Geology 104: 71-90.

Valentine, G., D. Krier, F. Perry, and G. Heiken 2005. Scoria cone construction mechanism, Lathrop Wells volcano southern Nevada, USA. Geology 33: 629-632.

Vergniolle, S. and M. Mangan 2000. Hawaiian and Strombolian eruptions. In: Encyclopedia of Volcanoes. Ed. H. Sigurdsson. Academic Press. p. 447.

Wilson, L., Sparks, R.S.J. and Walker, G.P.L., 1980. Explosive volcanic eruptions. IV. The control of magma properties and conduit geometry on eruption column behavior. Geophys. J. R. Astron. Soc. 63, p. 117-148.

Woods, A.W, S. Sparks, O. Bokhove, A. LeJeune, C. Connor, and B. Hill. Modeling magma-drift interaction at the proposed high-level radioactive waste repository at Yucca Mountain, Nevada, USA, *Geophysical Research Letters,* **13,** (2002).